PET/CT features of a novel gallium-68 labelled hypoxia seeking agent in patients diagnosed with tuberculosis: a proof-of-concept study

Bresser, Philippa L.[a,b,*]; Sathekge, Mike M.[a]; Vorster, Mariza[a,c]

[a]Department of Nuclear Medicine, Faculty of Health Sciences, University of Pretoria, Pretoria, South Africa

[b]Department of Anatomy and Medical Imaging, Faculty of Medical and Health Sciences, University of Auckland, Auckland, New Zealand

[c]Department of Nuclear Medicine, Inkosi Albert Luthuli Central Hospital, University of Kwazulu Natal, Durban, South Africa

*Correspondence to Philippa L. Bresser, PhD, Department of Nuclear Medicine, Faculty of Health Sciences, University of Pretoria, Steve Biko Academic Hospital, Level 5, Bridge A, Bophelo Road, Gezina, Pretoria 0002, South Africa, Tel: +64 204 091 2411; e-mail: pippa.bresser@auckland.ac.nz

Abstract

Introduction : Positron emission tomography/computed tomography (PET/CT) in infection and inflammation has yielded promising results across a range of radiopharmaceuticals. In particular, PET/CT imaging of tuberculosis (TB) allows for a better understanding of this complex disease by providing insights into molecular processes within the TB microenvironment. TB lesions are hypoxic with research primarily focussed on cellular processes occurring under hypoxic stress. With the development of hypoxia seeking PET/CT radiopharmaceuticals, that can be labelled in-house using a germanium-68/gallium-68 (^{68}Ge/^{68}Ga) generator, a proof-of-concept for imaging hypoxia in TB is presented.

Methods : Ten patients diagnosed with TB underwent whole-body PET/CT imaging, 60–90 min after intravenous administration of 74–185 MBq (2–5 mCi) ^{68}Ga-nitroimidazole. No oral or intravenous contrast was administered. Images were visually and semiquantitatively assessed for abnormal ^{68}Ga-uptake in the lungs.

Results : A total of 28 lesions demonstrating hypoxic uptake were identified. Low- to moderate-uptake was seen in nodules, areas of consolidation and cavitation as well as effusions. The mean standard uptake value (SUV_{mean}) of the lesions was 0.47 (IQR, 0.32–0.82) and SUV_{max} was 0.71 (IQR, 0.41–1.11). The lesion to muscle ratio (median, 1.70; IQR, 1.15–2.31) was higher than both the left ventricular and the aorta lesion to blood ratios.

Conclusion : Moving towards the development of unique host-directed therapies (HDT), modulation of oxygen levels may improve therapeutic outcome by reprogramming TB lesions to overcome hypoxia. This proof-of-concept study suggests that hypoxia in TB lesions can be imaged and quantified using ^{68}Ga-nitroimidazole PET/CT. Subsequently, hypoxic load can be estimated to inform personalised treatment plans of patients diagnosed with TB.

Keywords: ^{68}Ga-nitroimidazole, hypoxia, PET/computed tomography, tuberculosis

Introduction

Imaging plays an important role in the diagnosis and management of tuberculosis (TB) and the manifestations of TB using various imaging modalities such as x-rays [1], ultrasound [2,3], computed tomography (CT) and magnetic resonance imaging (MRI) [1,4] are well described. Although these imaging modalities provide excellent anatomic information, there is a lack of functional, metabolic or physiologic information. This gap has more recently been filled by the increased use of PET/CT in the diagnosis and management of infectious diseases. Molecular and cellular changes occur earlier than structural or anatomic changes in pathological processes. Therefore, molecular imaging provides the ideal opportunity in diagnosing and monitoring various disease states [5]. There has been increased utilisation of PET/CT in imaging TB with particular emphasis on the application of new radiopharmaceuticals or the repurposing of existing radiopharmaceuticals for diagnosis and patient management.

Tuberculous granulomas in guinea pigs, rabbits and nonhuman primates are hypoxic, and the hypoxic microenvironment is an important feature of TB lesions [6]. Belton *et al*. [7] found that TB lesions in humans are severely hypoxic when flourine-18 fluoromisonidazole (^{18}F-FMISO) PET/CT demonstrated heterogeneous uptake in hypoxic TB lesions within and between patients. Hypoxia leads to dormancy and latent disease [7,8]. Subsequently, dormant TB lesions become less susceptible to standard TB treatment regimens but have increased susceptibility to nitroimidazole drugs. This implies that PET/CT imaging with radiolabelled nitroimidazoles may identify patients who will benefit from alternative treatment strategies. Hypoxic PET/CT tracers have already been validated for the management of cancer and could play a role in the management of TB [8] by allowing for a better understanding of TB pathogenesis [7].

Gallium-68 (^{68}Ga)-labelled nitroimidazole derivatives have been synthesised and preclinically validated as promising candidates for hypoxia imaging [9–16]. ^{68}Ga-labelled nitroimidazoles demonstrated greater hydrophilicity, with faster clearance and increased target to background ratios compared with ^{18}F-labelled nitroimidazoles [9,13]. These characteristics make them ideal for hypoxia-specific imaging. Considering the hypoxic nature of TB lesions [7,17], the role of ^{68}Ga-labelled hypoxia-seeking agents may earn a place in the management of TB in an era shifting towards host-directed therapies (HDTs). The purpose of this study was to describe and quantify the hypoxic uptake of ^{68}Ga-nitroimidazole in patients diagnosed with TB as a proof-of-concept PET/CT study. This study was limited to lesions demonstrating hypoxic uptake in the lung only.

Methods

Patients were prospectively recruited from the hospital TB clinic register for this study. Eligible patients were identified after TB was confirmed by a combination of clinical history, positive bacteriologic test or culture and a chest x-ray (CXR). Patients were then invited to participate in the study. After providing informed consent, 10 patients underwent a whole-body (skull vertex to mid-thigh) ^{68}Ga-nitroimidazole PET/CT (Siemens Biograph 40, Erlangen, Germany) scan within a month after initiating TB therapy. Patients waited 60–90 min after administration of 74–185 MBq (2–5 mCi) ^{68}Ga-nitroimidazole intravenously before imaging commenced. The product (^{68}Ga-nitroimidazole) is not currently labelled for use as it is still investigational. No oral or intravenous contrast media was administered. Patients were positioned supine, head-first with both arms elevated where the patient condition allowed.

PET/CT images were acquired in three-dimensional mode with a 4-min emission scan over 7–9 PET bed positions and an image matrix of 512 × 512. Reconstruction of images with and without attenuation correction (CT based) was done using ordered subset expectation maximisation (OSEM) to yield axial, sagittal and coronal slices. Hypoxia in the lung lesions was analysed using Siemens E-Soft 4DM (Siemens) processing software. Corrected PET data were fused with the CT data. Images were visually assessed for abnormal radiolabelled nitroimidazole uptake in the lungs that corresponded with pathology observed on the CT. Manual 10-mm regions of interest (ROIs) were drawn in lesions demonstrating abnormal hypoxic tracer uptake. The standard uptake value (SUV), which is representative of the relative concentration of radiolabelled ^{68}Ga-nitroimidazole in the lesion of interest, normalised to the patient's weight and the dose of radiotracer administered (SUV = radiotracer activity x patient weight/injected dose) was recorded. A 10-mm ROI was drawn in the sternocleidomastoid muscle at the level of the hyoid bone to represent normoxic tissue as a background to calculate the lesion to muscle (background) ratios (LMRs) for all lesions. LMR is the preferred semiquantitative parameter to quantify the proportion of uptake in PET/CT hypoxia imaging [10–13,18,19]. Additional 10-mm circular ROIs were drawn in the left ventricle and aorta as blood surrogate regions to calculate the lesion to blood ratio (LBR_{LV} and LBR_{aorta}) [7,20,21]. Overall, 28 lesions demonstrating increased ^{68}Ga-nitroimidazole uptake were measured and used for this analysis. Descriptive data were analysed using IBM SPSS version 27 software (IBM Corp, Armonk, New York, USA) and summary statistics are presented below. Data were not normally distributed and are, thus, presented as medians with interquartile range (IQR). Approval to conduct the study was granted by the Research Ethics Committee of the Faculty of Health Sciences, University of Pretoria.

Results

Demographics and clinical presentation

The median age of the patients was 42 years (IQR, 30–52 years). Most of the patients were male (n = 6). More than half the patients (n = 6) had comorbid HIV.

The most common symptom reported before imaging included: coughing and weight loss (n = 9); fever and lethargy (n = 8) and chest pain (n = 4). Eight of the 10 patients were classified as a new diagnosis, whereas the remaining two were relapse patients. Patients were diagnosed with TB based on a combination of CXR, clinical data and bacteriologic confirmation.

Procedural

The median time between treatment initiation and imaging was 19 days (10–45 days). The median dose and volume, of ^{68}Ga-nitroimidazole administered, were 89.36 MBq (53.65–158.73 MBq) and 7.0 ml (5–10 ml), respectively. The pH of the product for injection was 6.0–7.4. The radiochemical purity determined ITLC-SG was 95–100%. Patients waited for an average of 89 min (IQR, 82–95 min) between injection and imaging.

PET/computed tomography findings

^{68}Ga-nitroimidazole showed high vascular activity with the kidneys being the primary route of excretion. Uptake was noted in the liver and intestines as reported preclinically [10–13,18,22]. All lesions that were measured, demonstrated low- to moderate-uptake in comparison to the background. All patients demonstrated hypoxic uptake in more than one TB lesion, although

some lung lesions noted on CT were not ^{68}Ga-nitroimidazole avid. The upper lobe was the most frequently affected. Various lesions including nodules, cavitation or consolidation (Fig. 1) throughout the lung fields demonstrated hypoxia. Two patients had associated pleural effusions which also demonstrated hypoxic uptake.

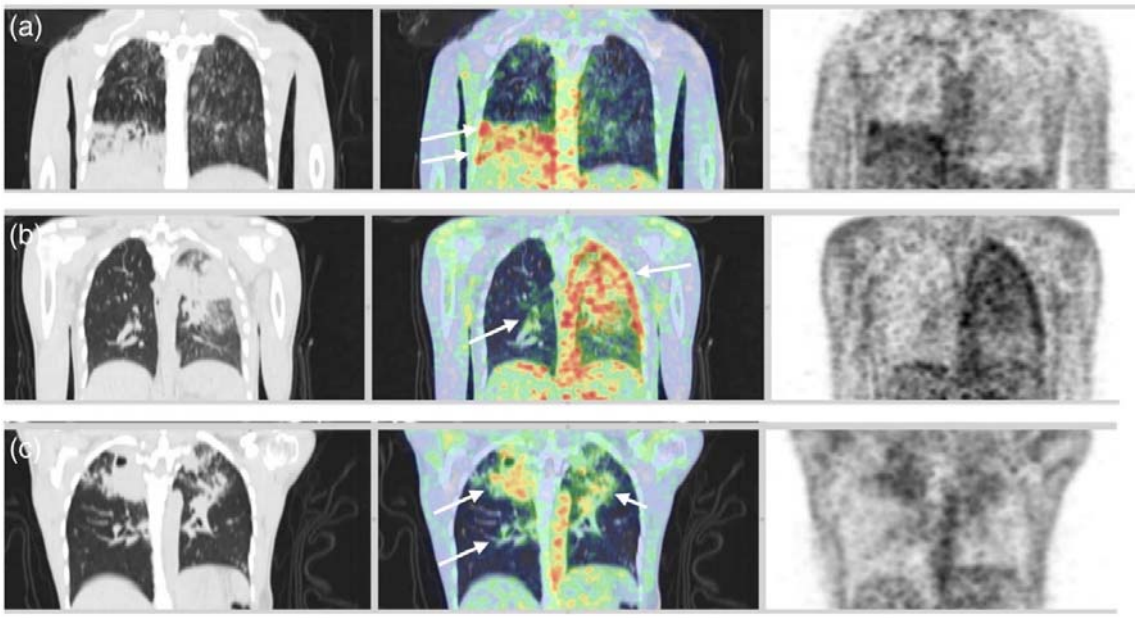

Fig. 1: Uptake of ^{68}Ga-nitroimidzole illustrated in: (a) 24-year-old male, 21 days after initiating therapy; (b) 27-year-old male, 31 days after commencing therapy; and (c) 32-year-old female, 15 days after initiating anti-TB therapy. ^{68}Ga, gallium-68; TB, tuberculosis.

Table 1 indicates the LMR of the lung lesions demonstrating hypoxic uptake of ^{68}Ga-nitroimidazole.

Table 1 - Summary of the tuberculosis lesions showing hypoxic uptake on the ^{68}Ga-nitroimidazole PET/CT

Lesion	Location	CT appearance	LMR
1	R upper lobe apical	Cavity	2.52
2	L apical	Fibrosis	3.10
3	R upper lobe superior (cavity rim)	Cavity	1.82
4	R upper lobe infero-posterior (cavity rim)	Cavity	2.09
5	R upper lobe infero-anterior (cavity rim)	Cavity	2.36
6	L upper lobe anterior segment	Cavity	1.36
7	R upper lobe	Consolidation with cavity	1.44
8	L upper lobe	Consolidation with cavity	1.33
9	L lower posterior	Nodule	1.03
10	L pleural effusion	Effusion	2.28
11	R upper lobe apical	Cavity	1.28
12	R upper lobe anterior segment along oblique fissure	Consolidation	1.16
13	R lower lobe medial basal	Consolidation	1.78
14	L lower lobe base	Fibrosis	1.56
15	R upper lobe apical segment	Nodule	2.73
16	L upper lobe apical segment	Nodule	2.68
17	L apico-posterior segment	Consolidation	1.72
18	L lower lingula	Consolidation	1.41
19	L middle lobe	Nodules	2.06
20	L pleural effusion	Effusion	3.16
21	R upper lobe anterior	Nodules	1.03
22	R middle lobe medial	Fibrosis	1.12
23	R middle lobe lateral	Fibrosis	1.11
24	R lower lobe	Consolidation	3.07
25	L apico-posterior	Cavity	2.29
26	L upper lobe apical infero-lateral	Cavity	1.68
27	R upper lobe cavity	Cavity	0.91
28	R superior segment of lower lobe posterior	Cavity	1.05

CT, computed tomography; L, left; LMR, lesion to muscle ratio; R, right.

The ROI SUVs for the lesions compared with the muscle as background are summarised in Table 2 as medians and IQRs due to the nonnormality of the data.

Table 2 - Standard uptake values of ^{68}Ga-nitroimidazole uptake in tuberculosis lung lesions and background

Region (10-mm ROI)	Median	IQR
Lesion SUV_{mean}	0.47	0.32–0.82
Lesion SUV_{max}	0.71	0.41–1.11
Muscle SUV_{mean}	0.32	0.22–0.36
Muscle SUV_{max}	0.50	0.31–0.69

IQR, interquartile range; ROI, regions of interest; SUV, standard uptake value.

Figure 2 illustrates the LMR according to the lesion type. For all lesions, the LMR was higher than both the left ventricle and aorta LBR.

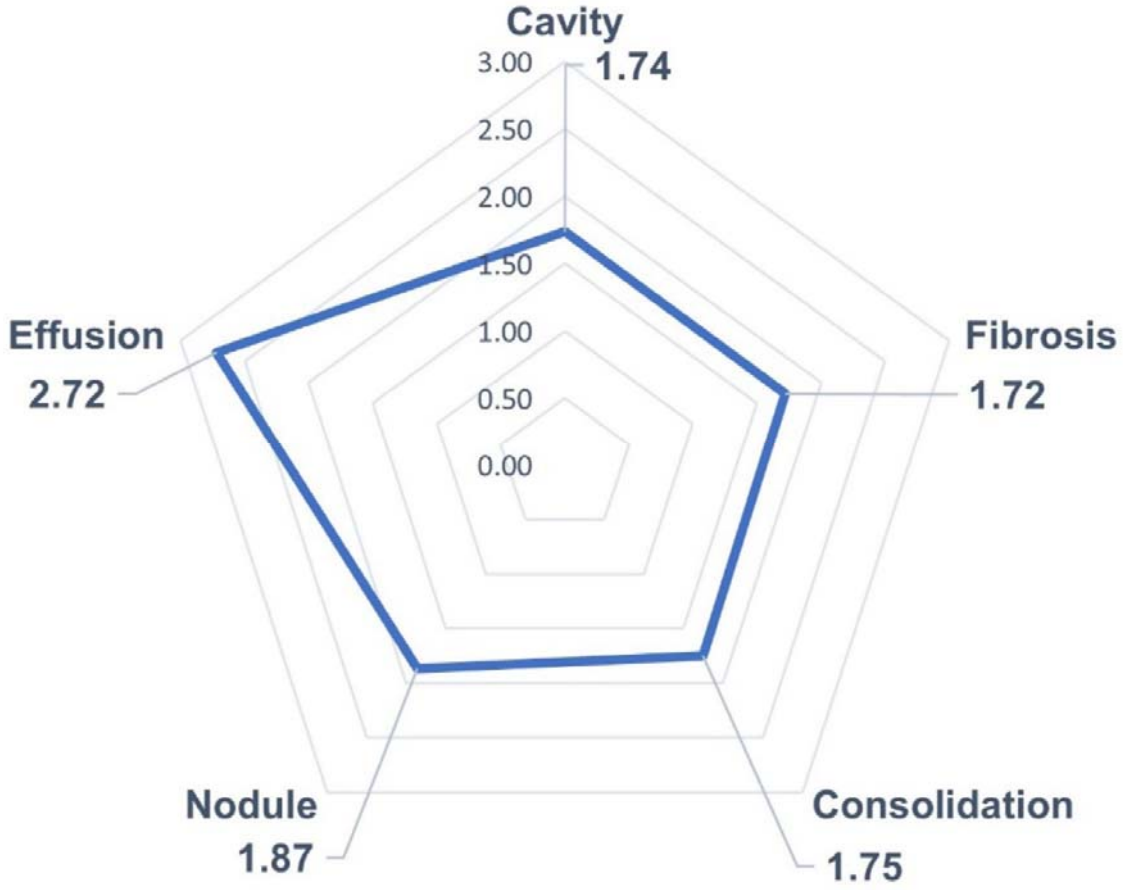

Fig. 2: Semi-quantitative ratios (LMR) of the ^{68}Ga-nitroimidazole uptake according to lesion type. ^{68}Ga, gallium-68; LMR, lesion to muscle ratio.

Discussion

Nuclear medicine and molecular imaging are increasingly being used in management of patients diagnosed with TB [1]. Hybrid imaging such as PET/CT has significant advantages over anatomic imaging [23], providing complementary physiological information about the disease [24,25]. The use of ^{18}F-FDG in TB diagnosis as well as monitoring and predicting treatment response have been well described [26–28] and summarised [29]. Although ^{18}F-FDG PET/CT is highly sensitive in detecting metabolic activity in infectious lesions, it still lacks specificity as uptake is also demonstrated in malignancies and inflammatory processes [5,30]. While the utilisation of ^{18}F-FDG in TB is well researched [27,31–34], other non-^{18}F-FDG PET/CT radiopharmaceuticals have also been explored. The role of ^{68}Ga-citrate [35,36], ^{11}C-choline [37], ^{11}C-labelled chemotherapeutics [38–40] and ^{68}Ga-labelled synthetic antimicrobial peptides in TB have been described [23]. Findings from these studies highlight the need to use PET/CT to understand the pathology and target-specific molecular processes in TB.

In the current proof-of-concept study, it is clear that TB hypoxia can indeed be imaged and quantified using PET/CT although uptake is of relatively low intensity. The low-intensity uptake aligns with other preclinical studies that investigated the use of ^{68}Ga-labelled

nitroimidazoles. Some pulmonary lesions did not display hypoxic uptake, which is consistent with the notion that the TB microenvironment varies significantly between and within lesions in a single host [7,41,42]. There was uptake noted outside the lung, in the mediastinum and shoulder joints of one patient. It could not be confirmed whether this uptake corresponded to infectious sites because no biopsy was performed and only lesions in the lung were analysed for this study. Comparative studies to ^{18}F-FDG and ^{18}F-FMISO may have been beneficial. Comparative PET/CT imaging was initially considered but abandoned in light of the cost and radiation exposure considerations. The unexpected uptake could be attributed to extrapulmonary lesions, because it is known that common sites of extrapulmonary TB include the pleura, lymph nodes, gastrointestinal and genitourinary organs, bones and joints and the central nervous system [43].

Tuberculosis as a bacterial tumour

In an effort to develop unique HDT to manage and eradicate TB, studies investigating the reprogramming of TB lesions to overcome hypoxia are underway [41,44,45]. The application of the term 'bacterial tumour' to TB seems well suited because the similarities between regulation of the human immune response to TB and solid tumours have recently been described [41,46]. Oehlers [47] explains that 'TB granulomas are structurally and molecularly similar to tumours'. Frank *et al*. [41] identify a common feature of both TB and solid tumours as having gradients of oxygen tension. It has been postulated that modulation of oxygen levels will improve therapeutic outcomes in TB [48] similar to the improved outcomes in cancer treatment once tumour hypoxia has been reduced [49]. The parallels drawn between TB and tumour vasculature, immunology, metabolism and tissue pathology suggest that reducing levels of hypoxia will make TB lesions more susceptible to TB chemotherapy [47]. Resistance of dormant bacteria in the hypoxic TB microenvironment [50] highlights the need to be able to image the hypoxic load [8] in TB lesions in order to determine whether the patient would benefit from alternative HDT as opposed to a standard treatment regimen.

There has been extensive use of hypoxia-seeking radiopharmaceuticals in oncology to plan therapy and monitor treatment response [51]. Hypoxia imaging with PET/CT plays a significant role in prognostic tumour imaging because the volume and intensity of hypoxia strongly correlate with disease progression, survival and prediction of relapse [51]. A similar strategy may be applicable in TB owing to the high specificity of hypoxia PET/CT as compared with other noninvasive hypoxia detection techniques [51]. Many authors have suggested that hypoxia plays a role in the host response to TB therapy [48]. Extending from this, the use of nitroimidazoles in TB therapy has been suggested with the emergence of new HDTs being explored as well as repurposing 'old' drugs to refine treatment on a case-by-case basis [52–54].

The use of nitroimidazoles such as ^{18}F-FMISO, ^{18}F-fluoroazomycinarabinozide (^{18}F-FAZA), ^{18}F-fluoroerythron-itroimidazole (^{18}F-FETNIM), ^{18}F-2-nitroimidazol-pentafluoropropyl acetamide (^{18}F-EF5) and ^{124}I-iodoazomycin galactopyranoside (^{124}I-IAGZ), among others, have been explored for potential use in tumours [51]. Their application can be paralleled for use in TB as illustrated by Belton *et al*. [7]. The limitations of ^{18}F-labelled hypoxia-seeking agents include the high background and slow selective uptake due to their lipophilic nature. ^{18}F-labelled agents also requires readily available and reliable supply from a cyclotron facility. An in-house bench-top germanium-68/gallium-68 (^{68}Ge/^{68}Ga) generator provides a more feasible option for hypoxia imaging with labelling processes on site [55]. Since ^{68}Ga-nitroimidazoles are more hydrophilic [9,13], compared with ^{18}F-FMISO, it was anticipated that

the LMR would be higher in the current study and that uptake would be more intense [13]. However, the findings align with Wu *et al*. [14], who raised the concern that the hydrophilicity may lead to insufficient retention and accumulation in hypoxic cells [14]. Furthermore, hypoxia PET/CT is known to have inherently low signal-to-noise ratios [56]. One should also consider the different intrinsic physical characteristics between ^{68}Ga and ^{18}F, which ultimately affect the spatial resolution and sensitivity of PET/CT images [57,58].

Quantifying hypoxia and comparison to preclinical studies

The selective entrapment of nitroimidazoles within regions of hypoxia allows for quantitative estimates of hypoxia in tissue using PET/CT [59]. Many different approaches have been used in reporting uptake of hypoxia-seeking radiopharmaceuticals. The most common semiquantitative measures used in addition to the SUV to report hypoxic:normoxic tissue is the lesion (or tumour) to muscle and lesion (or tumour) to blood ratio. Carlin and Humm [59] state that for studies that used ^{18}F-labelled hypoxic agents, activity concentrations greater than 1.3 times the concentration in blood reflect locoregional hypoxia. In another study with ^{18}F-MISO, a tumour to muscle ratio of 1.4 was indicative of hypoxia 2 h after injection [4]. In-vitro results indicate a hypoxic:normoxic ratio of 6:1. Since hypoxia exists in a transient and variable state within single lesions, individual PET voxels will typically only reflect 5–30% hypoxic tissue. Therefore, it is more appropriate to expect a 2:1 ratio indicative of hypoxia [59]. Preclinical studies report hypoxic:normoxic ratios for ^{68}Ga-labelled radiopharmaceuticals ranging from 1.8 to 7.9 depending on the nitroimidazole derivative and tumour cell line that was used [10–12,16]. These studies also report LMRs ranging from 1.41 to 5.7 and LBRs from 0.6 to 1.5 [10–13,18]. Our results align with these semiquantitative preclinical studies. Fernández *et al*. [9] concluded the ^{68}Ga-nitroimidazole derivatives from their study yielded results comparable to ^{18}F-FMISO with favourable biodistribution and LMRs. Although, head-to-head comparison to other studies is challenging due to differences in PET hardware, image reconstruction, processing, radiopharmaceutical used and semiquantitative analysis; the use of ^{68}Ga-nitroimidazoles provides a viable option for hypoxia imaging with PET/CT. Overall, the ^{68}Ga-nitroimidazole uptake in TB lesions demonstrated low intensity. This is consistent with studies that used ^{18}F-labelled nitroimidazoles in oncologic studies [51] and with ^{68}Ga-nitroimidazole preclinical uptake data [10,12,13,16].

Conclusion

^{68}Ga-nitroimidazole yielded relatively low-grade uptake with a SUV_{mean} of 0.47 (IQR, 0.32–0.82) and LMR of 1.70 (IQR, 1.15–2.31) in lung lesions of patients diagnosed with TB. The LMR appears to be the most favourable quantification method. The results from this proof-of-concept study suggest that hypoxia in TB lesions can be imaged using ^{68}Ga-nitroimidazole PET/CT. Furthermore, the hypoxia can be described and quantified to identify patients that may benefit from nitroimidazoles as part of HDT. Early determination of hypoxic load in patients diagnosed with TB will enable the identification of the extent of lesions that could harbour dormant bacilli. Being aware that the patient has lesions potentially resistant to current anti-TB drugs and, thus, the potential for long treatment durations, relapse or the development of latent TB, we can harness the potential power of individualised patient treatment and adjunctive therapies towards the goal of TB eradication. A robust clinical trial using ^{68}Ga-nitroimidazole PET/CT to image TB hypoxia is needed to determine the impact on patient management and whether the hypoxic load can be used to predict treatment

outcome at an early stage. In addition, the potential of ^{68}Ga-nitroimidazole imaging in other infectious diseases should be explored.

Conflicts of interest

There are no conflicts of interest.

References

1. Bomanji JB, Gupta N, Gulati P, Das CJ. Imaging in tuberculosis. Cold Spring Harb Perspect Med 2015; 5:a017814.
2. Ladumor H, Al-Mohannadi S, Ameerudeen FS, Ladumor S, Fadl S. TB or not TB: a comprehensive review of imaging manifestations of abdominal tuberculosis and its mimics. Clin Imaging 2021; 76:130–143.
3. Bigio J, Kohli M, Klinton JS, MacLean E, Gore G, Small PM, et al. Diagnostic accuracy of point-of-care ultrasound for pulmonary tuberculosis: a systematic review. PLoS One 2021; 16:e0251236.
4. Challapalli A, Carroll L, Aboagye EO. Molecular mechanisms of hypoxia in cancer. Clin Transl Imaging 2017; 5:225–253.
5. Gordon O, Ruiz-Bedoya CA, Ordonez AA, Tucker EW, Jain SK. Molecular imaging: a novel tool to visualize pathogenesis of infections in situ. mBio 2019; 10:e00317–e00319.
6. Via LE, Lin PL, Ray SM, Carrillo J, Allen SS, Eum SY, et al. Tuberculous granulomas are hypoxic in guinea pigs, rabbits, and nonhuman primates. Infect Immun 2008; 76:2333–2340.
7. Belton M, Brilha S, Manavaki R, Mauri F, Nijran K, Hong YT, et al. Hypoxia and tissue destruction in pulmonary TB. Thorax 2016; 71:1145–1153.
8. Ankrah AO, Glaudemans AW, Sathekge MM, Klein HC. Imaging latent tuberculosis infection with radiolabeled nitroimidazoles. Clin Transl Imaging 2016; 4:157–159.
9. Fernández S, Dematteis S, Giglio J, Cerecetto H, Rey A. Synthesis, *in vitro* and *in vivo* characterization of two novel 68Ga-labelled 5-nitroimidazole derivatives as potential agents for imaging hypoxia. Nucl Med Biol 2013; 40:273–279.
10. Hoigebazar L, Jeong JM, Hong MK, Kim YJ, Lee JY, Shetty D, et al. Synthesis of 68Ga-labeled DOTA-nitroimidazole derivatives and their feasibilities as hypoxia imaging PET tracers. Bioorg Med Chem 2011; 19:2176–2181.
11. Hoigebazar L, Jeong JM, Choi SY, Choi JY, Shetty D, Lee YS, et al. Synthesis and characterization of nitroimidazole derivatives for 68Ga-labeling and testing in tumor xenografted mice. J Med Chem 2010; 53:6378–6385.
12. Seelam SR, Lee JY, Lee YS, Hong MK, Kim YJ, Banka VK, et al. Development of 68Ga-labeled multivalent nitroimidazole derivatives for hypoxia imaging. Bioorg Med Chem 2015; 23:7743–7750.
13. Sano K, Okada M, Hisada H, Shimokawa K, Saji H, Maeda M, Mukai T. *In vivo* evaluation of a radiogallium-labeled bifunctional radiopharmaceutical, Ga-DOTA-MN2, for hypoxic tumor imaging. Biol Pharm Bull 2013; 36:602–608.
14. Wu Y, Hao G, Ramezani S, Saha D, Zhao D, Sun X, Sherry AD. [68Ga]-HP-DO3A-nitroimidazole: a promising agent for PET detection of tumor hypoxia. Contrast Media Mol Imaging 2015; 10:465–472.
15. Kilian K. 68Ga-DOTA and analogs: current status and future perspectives. Rep Pract Oncol Radiother 2014; 19:S13–S21.

16. Ramogida CF, Pan J, Ferreira CL, Patrick BO, Rebullar K, Yapp DT, et al. Nitroimidazole-containing H2dedpa and H2CHXdedpa derivatives as potential PET imaging agents of hypoxia with 68Ga. Inorg Chem 2015; 54:4953–4965.
17. Tsai MC, Chakravarty S, Zhu G, Xu J, Tanaka K, Koch C, et al. Characterization of the tuberculous granuloma in murine and human lungs: cellular composition and relative tissue oxygen tension. Cell Microbiol 2006; 8:218–232.
18. Leung K. 68Ga-1,4,7-Triazacyclononane-1,4,7-triacetic acid-2-nitroimidazole-N-ethylamine. In: Molecular Imaging and Contrast Agent Database (MICAD) [Internet]. National Center for Biotechnology Information (Bethesda, US); 2004 [updated 23 March 2011 (Accessed 12 March 2018)].
19. Mokoala KMG, Lawal IO, Jeong JM, Sathekge MM, Vorster M. Radionuclide imaging of hypoxia: where are we now? Special attention to cancer of the cervix uteri. Hell J Nucl Med 2021; 24:247–261.
20. Mönnich D, Welz S, Thorwarth D, Pfannenberg C, Reischl G, Mauz PS, et al. Robustness of quantitative hypoxia PET image analysis for predicting local tumor control. Acta Oncol 2015; 54:1364–1369.
21. Taylor E, Yeung I, Keller H, Wouters BG, Milosevic M, Hedley DW, Jaffray DA. Quantifying hypoxia in human cancers using static PET imaging. Phys Med Biol 2016; 61:7957–7974.
22. Bresser PL, Vorster M, Sathekge MM. An overview of the developments and potential applications of 68Ga-labelled PET/CT hypoxia imaging. Ann Nucl Med 2021; 35:148–158.
23. Ferro-Flores G, Avila-Rodríguez MA, García-Pérez FO. Imaging of bacteria with radiolabeled Ubiquicidin by SPECT and PET techniques. Clin Transl Imaging. 2016; 4:175–82.
24. Jain SK. The promise of molecular imaging in the study and treatment of infectious diseases. Mol Imaging Biol 2017; 19:341–347.
25. Johnson DH, Via LE, Kim P, Laddy D, Lau CY, Weinstein EA, Jain S. Nuclear imaging: a powerful novel approach for tuberculosis. Nucl Med Biol 2014; 41:777–784.
26. Soussan M, Brillet PY, Mekinian A, Khafagy A, Nicolas P, Vessieres A, Brauner M. Patterns of pulmonary tuberculosis on FDG-PET/CT. Eur J Radiol 2012; 81:2872–2876.
27. Lawal IO, Fourie BP, Mathebula M, Moagi I, Lengana T, Moeketsi N, et al. 18F-FDG PET/CT as a noninvasive biomarker for assessing adequacy of treatment and predicting relapse in patients treated for pulmonary tuberculosis. J Nucl Med 2020; 61:412–417.
28. Yu W-Y, Lu P-X, Assadi M, Huang X-L, Skrahin A, Rosenthal A, et al. Updates on 18F-FDG-PET/CT as a clinical tool for tuberculosis evaluation and therapeutic monitoring. Quant Imaging Med Surg. 2019; 9:1132–1146.
29. Ankrah AO, van der Werf TS, de Vries EF, Dierckx RA, Sathekge MM, Glaudemans AW. PET/CT imaging of mycobacterium tuberculosis infection. Clin Transl Imaging 2016; 4:131–144.
30. Malherbe ST, Chen RY, Dupont P, Kant I, Kriel M, Loxton AG, et al. Quantitative 18F-FDG PET-CT scan characteristics correlate with tuberculosis treatment response. EJNMMI Res 2020; 10:8.
31. Chen RY, Dodd LE, Lee M, Paripati P, Hammoud DA, Mountz JM, et al. PET/CT imaging correlates with treatment outcome in patients with multidrug-resistant tuberculosis. Sci Transl Med 2014; 6:265ra166.

32. Vorster M, Sathekge MM, Bomanji J. Advances in imaging of tuberculosis: the role of ^{18}F-FDG PET and PET/CT. Curr Opin Pulm Med 2014; 20:287–293.
33. Bomanji J, Sharma R, Mittal BR, Gambhir S, Qureshy A, Begum SMF, et al.; International Atomic Energy Agency Extra-pulmonary TB Consortium. PET/CT features of extrapulmonary tuberculosis at first clinical presentation: a cross-sectional observational 18F-FDG imaging study across six countries. Eur Respir J 2020; 55:1901959.
34. Heysell SK, Thomas TA, Sifri CD, Rehm PK, Houpt ER. 18-Fluorodeoxyglucose positron emission tomography for tuberculosis diagnosis and management: a case series. BMC Pulm Med 2013; 13:14.
35. Vorster M, Maes A, Wiele Cv, Sathekge M. Gallium-68 PET: a powerful generator-based alternative to infection and inflammation imaging. Semin Nucl Med 2016; 46:436–447.
36. Vorster M, Maes A, Jacobs A, Malefahlo S, Pottel H, Van de Wiele C, Sathekge MM. Evaluating the possible role of 68Ga-citrate PET/CT in the characterization of indeterminate lung lesions. Ann Nucl Med 2014; 28:523–530.
37. Hara T, Kosaka N, Suzuki T, Kudo K, Niino H. Uptake rates of 18F-fluorodeoxyglucose and 11C-choline in lung cancer and pulmonary tuberculosis: a positron emission tomography study. Chest 2003; 124:893–901.
38. Ordonez AA, Wang H, Magombedze G, Ruiz-Bedoya CA, Srivastava S, Chen A, et al. Dynamic imaging in patients with tuberculosis reveals heterogeneous drug exposures in pulmonary lesions. Nat Med 2020; 26:529–534.
39. Liu L, Xu Y, Shea C, Fowler JS, Hooker JM, Tonge PJ. Radiosynthesis and bioimaging of the tuberculosis chemotherapeutics isoniazid, rifampicin and pyrazinamide in baboons. J Med Chem 2010; 53:2882–2891.
40. Tucker EW, Guglieri-Lopez B, Ordonez AA, Ritchie B, Klunk MH, Sharma R, et al. Noninvasive 11C-rifampin positron emission tomography reveals drug biodistribution in tuberculous meningitis. Sci Transl Med 2018; 10:eaau0965.
41. Frank DJ, Horne DJ, Dutta NK, Shaku MT, Madensein R, Hawn TR, et al. Remembering the host in tuberculosis drug development. J Infect Dis 2019; 219:1518–1524.
42. Heng Y, Seah PG, Siew JY, Tay HC, Singhal A, Mathys V, et al. Mycobacterium tuberculosis infection induces hypoxic lung lesions in the rat. Tuberculosis (Edinb) 2011; 91:339–341.
43. Lee JY. Diagnosis and treatment of extrapulmonary tuberculosis. Tuberc Respir Dis (Seoul) 2015; 78:47–55.
44. Tsenova L, Singhal A. Effects of host-directed therapies on the pathology of tuberculosis. J Pathol 2020; 250:636–646.
45. Kim YR, Yang CS. Host-directed therapeutics as a novel approach for tuberculosis treatment. J Microbiol Biotechnol 2017; 27:1549–1558.
46. Bickett TE, Karam SD. Tuberculosis-cancer parallels in immune response regulation. Int J Mol Sci 2020; 21:E6136.
47. Oehlers Stefan H. Revisiting hypoxia therapies for tuberculosis. Clin Sci 2019; 133:1271–1280.
48. Baer CE, Rubin EJ, Sassetti CM. New insights into TB physiology suggest untapped therapeutic opportunities. Immunol Rev 2015; 264:327–343.
49. Phillips RM. Targeting the hypoxic fraction of tumours using hypoxia-activated prodrugs. Cancer Chemother Pharmacol 2016; 77:441–457.
50. Ankrah AO, Glaudemans AWJM, Maes A, Van de Wiele C, Dierckx RAJO, Vorster M, Sathekge MM. Tuberculosis. Semin Nucl Med 2018; 48:108–130.

51. Lopci E, Grassi I, Chiti A, Nanni C, Cicoria G, Toschi L, et al. PET radiopharmaceuticals for imaging of tumor hypoxia: a review of the evidence. Am J Nucl Med Mol Imaging 2014; 4:365–384.
52. Mukherjee T, Boshoff H. Nitroimidazoles for the treatment of TB: past, present and future. Future Med Chem 2011; 3:1427–1454.
53. Ang CW, Jarrad AM, Cooper MA, Blaskovich MAT. Nitroimidazoles: molecular fireworks that combat a broad spectrum of infectious diseases. J Med Chem 2017; 60:7636–7657.
54. Dawson R, Harris K, Conradie A, Burger D, Murray S, Mendel C, et al. Efficacy of bedaquiline, pretomanid, moxifloxacin & PZA (BPAMZ) against DS-& MDR-TB. Conference on Retroviruses and Opportunistic Infections (CROI); CROI Foundation in partnership with the International Antiviral Society-USA; 2017.
55. Jalilian AR. An overview on Ga-68 radiopharmaceuticals for positron emission tomography applications. Iranian J Nucl Med 2016; 24:1–10.
56. Wack LJ, Mönnich D, van Elmpt W, Zegers CM, Troost EG, Zips D, Thorwarth D. Comparison of [18F]-FMISO, [18F]-FAZA and [18F]-HX4 for PET imaging of hypoxia–a simulation study. Acta Oncol 2015; 54:1370–1377.
57. Kim JH, Lee JS, Kim JS, Chung J-K, Lee MC, Lee DS. Physical performance comparison of Ga-68 and F-18 in small animal PET system. J Nucl Med 2010; 51(Suppl 2):1423.
58. Naftalin CM, Leek F, Hallinan JTPD, Khor LK, Totman JJ, Wang J, et al. Comparison of 68Ga-DOTANOC with 18F-FDG using PET/MRI imaging in patients with pulmonary tuberculosis. Sci Rep 2020; 10:14236.
59. Carlin S, Humm JL. PET of hypoxia: current and future perspectives. J Nucl Med 2012; 53:1171–1174.